ELSEVIER

Contents lists available at SciVerse ScienceDirect

## Journal of Biomechanics

journal homepage: www.elsevier.com/locate/jbiomech www.JBiomech.com



# Stress profile of infant rib in the setting of child abuse: A finite element parametric study

Andy Tsai a,\*, Brittany Coats b, Paul K. Kleinman a

- <sup>a</sup> Department of Radiology, Children's Hospital Boston, Harvard Medical School, 300 Longwood Avenue, Boston, MA 02115, United States
- b Department of Mechanical Engineering, University of Utah, Salt Lake City, UT, United States

#### ARTICLE INFO

Article history: Accepted 19 May 2012

Keywords:
Finite element model
Lateral grip
Parametric analysis
Child abuse
Infant rib fracture

#### ABSTRACT

The primary goal of this study is to advance our current understanding of infant rib injuries in the setting of child abuse. To this end, we employed finite element model simulations to determine the sensitivity of an infant rib's stress response to varying material properties and under varying degrees of anterior-posterior chest compression. Using high-resolution chest CT images obtained from a 6-dayold infant, we constructed a simplified geometric model consisting of bone and cartilage structures. To simulate the lateral gripping of an infant in child abuse, an anterior-posterior chest compression load was applied to cause increased stresses along the costovertebral articulation, a classic site for inflicted rib fractures. A sensitivity analysis was conducted to quantify the effects of varying Young's modulus and Poisson's ratio of the bones and cartilages. In addition, we varied the amount of anteriorposterior chest displacement to assess the sensitivity of this parameter to the rib's stress profile. We found that varying Young's modulus of the bone and cartilage not only changed the magnitude but also the shape profile of the rib's stress response. In contrast, varying the degree of chest compression only changed the magnitude of the stress response and not the shape profile. We also discovered that by varying Poisson's ratio of the bone and cartilage, no appreciable change was seen in the magnitude or the shape profile of the rib's stress response. Finite element modeling shows promise as a tool to elucidate the mechanisms of rib fractures in abused infants.

© 2012 Elsevier Ltd. All rights reserved.

#### 1. Introduction

Unlike adults, in whom rib fractures are frequent and often caused by direct impact, rib fractures in infancy ( $\leq 12$  months old) are uncommon and often caused by child abuse (Worn and Jones, 2007). Although direct impact may occasionally play a role, manual thoracic compression is generally assumed to be the cause of most inflicted infant rib fractures (Betz and Liebhardt, 1994; Kleinman, 1990; Kleinman et al., 1996; Kleinman and Schlesinger, 1997; Reece, 1993, 2002, Worn and Jones, 2007). Fractures near the costovertebral articulations are highly associated with infant abuse, and although anterior-posterior compression of the rib cage during assaults is supported by perpetrator confessions and injury morphology, rigorous laboratory research that characterizes the type and magnitude of force required to cause inflicted rib fractures is lacking (Boal, 2008; Kleinman, 1990; Lonergan et al., 2003; Reece, 1993). Attempts to understand infant rib fracture with in vivo experimentation are not feasible. Finite element (FE) modeling offers an attractive alternative to develop a scientific foundation for investigating these theories. Thus, the goal of this paper is to begin the development of an FE model that can be used to advance our current understanding of infant rib fractures and better understand the biomechanical response of infant ribs during child abuse.

While there are numerous reports of the biomechanical response of adult ribs under stress using the FE modeling (Charpail et al., 2005; Ito et al., 2009; Kemper et al., 2005; Li et al., 2010a, 2010b; Niu et al., 2007; Ruan et al., 2003; Yoganandan and Pintar, 1998), similar information on infant ribs is lacking, mostly because there is very little material property data on infant ribs. To our knowledge, there is only one study that reported the material properties of pediatric ribs (Pfefferle et al., 2007). In that study, Young's modulus, yield force, and rib stiffness of the pediatric rib bone were explored in 13 subjects ranging in age from 1-day-old to 72-months-old. As is typical in studies with limited human specimen availability, variability is large and identifying representative properties for the FE modeling is challenging. Therefore, the objective of this study was to identify the material properties that most influence the infant rib stress response during abusive chest compression, and ascertain whether changes in chest compression depth significantly alter patterns of stress. These findings will provide preliminary data that can direct future research for predicting rib fracture in children.

<sup>\*</sup> Corresponding author. Tel.: +1 857 218 5102; fax: +1 617 730 0635. E-mail address: andy.tsai@childrens.harvard.edu (A. Tsai).

#### 2. Methods

#### 2.1. Geometry

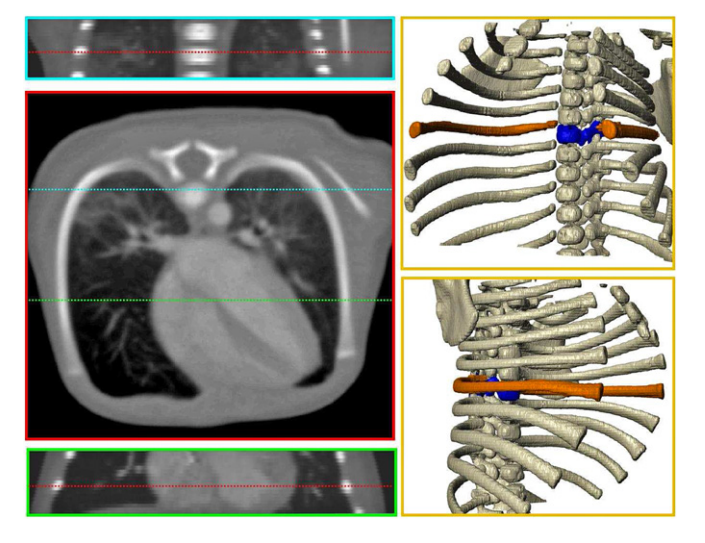
For anatomic fidelity of an infant's chest, the geometry of the FE rib model was constructed based on a chest CT of a 6-day-old boy (approved by the Institutional Review Board at Children's Hospital Boston), with  $0.28 \times 0.28$  mm in-plane resolution, 2 mm slice thickness, 80 KVp, 90 mAs, and pitch of 1. This chest CT, acquired on a Siemens Sensation 64 multi-detector CT (Siemens Medical Solutions, Malvern, PA), was initially performed to investigate a small lucent lung lesion found on a chest radiograph taken in the setting of respiratory distress. This lucent lesion was found to represent a small loculated pneumothorax that resolved on a follow up study.

The FE model was focused on a single rib pair, as a high-resolution model consisting of the entire rib cage and associated soft tissue would be computationally intractable. The FE geometry was derived by using a semiautomated segmentation algorithm, which included a combination of intensity thresholding (>120/255), 3D region growing, morphologic filtering, and 3D Gaussian smoothing to outline the smooth bony contour of the sixth rib and vertebral body (ScanIP, Simpleware Ltd., Exeter, UK). The sixth rib was selected because this is a "true" rib and most rib fractures in abused infants occur in the mid portion of the rib cage (Kleinman et al., 2000). The rib bone was modeled as a homogeneous solid structure without separating it into cortical and trabecular components due to the poor spatial resolution of CT in differentiating these components (Fig. 1). The sixth rib pair in infants is relatively horizontal and planar in configuration compared to adult rib pairs (Openshaw et al., 1984). The contours of the cartilage structures (inter-vertebral disks, anterior costal cartilage, rib head and transverse process cartilage apophyses, and vertebral synchondroses cartilage) could not be identified on CT; hence, these structures were created based on anatomical atlases (Gray, 1974; Netter, 2003). The sternum at the level of the sixth rib is cartilaginous and has not yet ossified at this age.

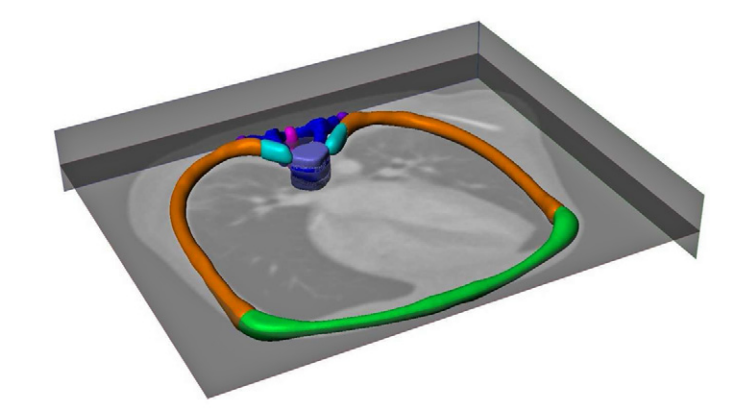
The final  $442 \times 363 \times 64$  voxel model had an isotropic voxel resolution of 0.28 mm (Fig. 2). The sixth rib was approximately 8.4 cm long. The anterior-posterior diameter of the thorax was 9.2 cm. The circumference of the thorax, including the overlying soft tissue, was 33.5 cm. The model had a slight right-left asymmetry that is within the range of normal anatomic variability.

#### 2.2. Material properties

For simplicity, bone and cartilage were modeled as isotropic elastic materials using Navier–Cauchy equations. As such, Poisson's ratio and Young's modulus *E* were necessary components for the FE simulations. A FE parametric study was performed to determine the influence of Young's modulus and Poisson's ratio of



**Fig. 1.** Chest CT and 3D rendering of a 6-day-old infant's bony thorax. The axial and coronal CT images along the left column illustrate the bone density along the axial and coronal planes of the infant's 6th rib. Notice the poor spatial differentiation between the bone's cortex and trabecula due to its diminutive size. The right column demonstrates two 3D renderings of the bony thorax based on the chest CT. The paired sixth rib is outlined in orange, while the sixth vertebral body is outlined in blue. Notice the relatively planar and horizontal configuration of the rib pairs, with the sixth rib pair oriented nearly perpendicular to the axis of the spine. (For interpretation of the references to color in this figure legend, the reader is referred to the web version of this article.)



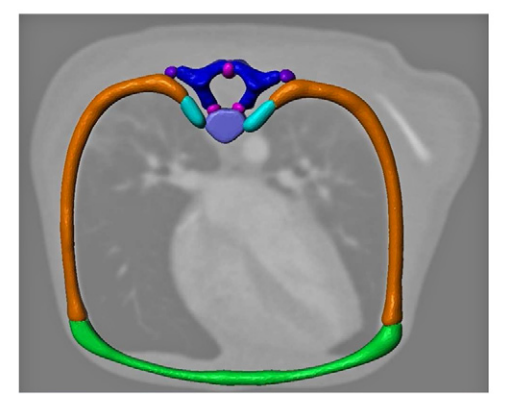


**Fig. 2.** Two views of the single rib pair model. In keeping with anatomic imaging, the right rib is to the left of the image while the left rib is to the right of the image. The anatomic structures include paired sixth rib (orange), sixth vertebral body (dark blue), inter-vertebral disks (light purple), rib head cartilage apophyses (cyan), transverse process cartilage apophyses (dark purple), vertebral synchondroses cartilage (magenta), and anterior costal cartilage (green). (For interpretation of the references to color in this figure legend, the reader is referred to the web version of this article.)

bone and cartilage on stress magnitude and distribution during infant chest compression. We chose to evaluate von Mises stress  $\sigma_{vm}$  for analysis.

#### 2.2.1. Bone

The same material properties were assigned to the rib and vertebral body. A low, baseline, and high value were used for each of the properties.

Young's modulus. The baseline value was chosen based on the following nonlinear relationship between Young's modulus of cortical bone and biological age developed by Pfefferle et al. (2007):

$$E = 138.99x^{0.7996} \tag{1}$$

where x is the age in months. Using this equation, we estimated the baseline modulus of a 6-day-old infant to be 38 MPa. Because there was a significant amount of variability in the pediatric rib measurements, the low value for the modulus (9 MPa) was obtained by plugging the biological age of 1-day (the youngest specimen in that study) into Eq. (1). The high value for the modulus (9 GPa) was the largest data point provided in Pfefferle's study.

Poisson's ratio. The baseline value for Poisson's ratio was set at 0.379, which is the average value from adult rib bone (Abe et al., 1996; Greer, 2006; Viano, 1986). The low value for Poisson's ratio (0.3) was Poisson's ratio of the adult cortical bone (Li et al., 2010a, 2010b). By purposely choosing Poisson's ratio of the cortical bone (which is harder and denser than trabecular bone), we positioned ourselves at the low end of the scale for this parameter. Using a similar argument, the high value for Poisson's ratio (0.45) was Poisson's ratio of the adult trabecular bone (Li et al., 2010a, 2010b).

#### 2.2.2. Cartilage

The same properties were assigned to all the cartilage structures. A low, baseline, and high value were used for each of the properties.

Young's modulus. The baseline value for Young's modulus (2.3 MPa) is the modulus reported for a 3-year-old child's cartilage (Mizuno et al., 2005). While this measurement reflects that of a toddler, it remains the nearest approximation in age (found in the literature) to the 6-day-old infant selected for our study. The low value for the modulus (0.06 MPa) is representative of the cartilage anlagen of

### Download English Version:

# https://daneshyari.com/en/article/872754

Download Persian Version:

https://daneshyari.com/article/872754

Daneshyari.com